European Journal of Pharmaceutics and Biopharmaceutics 80 (2012) 217–225

Contents lists available at SciVerse ScienceDirect

European Journal of Pharmaceutics and Biopharmaceutics

journal homepage: www.elsevier.com/locate/ejpb

Research paper

Addressing potent single molecule AFM study in prediction of swelling and dissolution rate in polymer matrix tablets

Biljana Govedarica [a,*], Tamás Sovány [b], Klara Pintye-Hódi [b], Miha Škarabot [c], Saša Baumgartner [a], Igor Muševič [c], Stane Srčič [a]

[a] Department of Pharmaceutical Technology, University of Ljubljana, Ljubljana, Slovenia
[b] Department of Pharmaceutical Technology, University of Szeged, Szeged, Hungary
[c] Department of Condensed Matter Physics, Jožef Stefan Institute, Ljubljana, Slovenia

ARTICLE INFO

Article history:
Received 3 July 2011
Accepted in revised form 12 September 2011
Available online 21 September 2011

Keywords:
AFM
Xanthan
Single molecule
Nanoindentation
Matrix tablets
Swelling

ABSTRACT

Our goal was to understand and thus be able to predict the swelling behavior of xanthan matrix tablets in media of various pH and ionic strengths using data obtained from single xanthan molecules and films with atomic force microscopy.

Imaging was performed in 1-butanol using contact mode AFM in order to characterize single xanthan chains prepared from various solutions. Image analysis was used to calculate the molecular contour, persistence length, and radius of gyration. Nanoindentation measurements of xanthan films were carried out to evaluate their mechanical properties. Increasing the ionic strength of solutions induced reductions in chain parameters such as molecular contour, persistence length, and radius of gyration. Nanomechanical measurements demonstrated that Young's moduli of xanthan films prepared from solutions with higher ionic strengths are twice as large as those prepared at lower ionic strengths. This may help explain xanthan matrix tablets' reduced degree of swelling and faster dissolution rate in the presence of salts or ions. We successfully come to conclusion that microscopic polymer properties such as radius of gyration and persistence length are responsible for the macroscopic polymer behavior. For instance, longer persistence lengths and radius of gyration of xanthan's chains result in a higher degree of swelling, corresponding to softer polymer films, increased gel layers in matrix, and a slower release rate of the incorporated drug from the tablets.

1. Introduction

Drug delivery is an important drug life-cycle management tool. Controlled-release technology (CRT) evolved in the 1950s with matrix technology in order to achieve a constant release rate of the incorporated drug. Since that time, the industry has invented a number of innovative oral controlled-release dosage forms, with new patents being awarded at a rapid pace. Recent advances in oral CRT are mostly attributed to the development and implementation of novel biocompatible polymers. To date, the main drug-delivery approach that has seen ongoing success over time has been the matrix systems made of swellable and non-swellable polymers [1].

Xanthan gum (Xan) is one of the most-used hydrocolloids in the pharmaceutical industry. There are various reasons for this, but it is usually utilized alone or in combination with other polysaccharides as a controlled-release matrix constituent [2]. Its primary structure is presented in Fig. 1a. The presence of glucuronic acid as well as the pyruvate acid groups in the Xan molecule is mainly responsible for its anionic character (Fig. 1a) [3,4].

Xan adopts a helical structure in order to reduce steric and electrostatic repulsions between the charged groups in side chains. This is schematically represented in Fig. 1b [5].

Polysaccharides exhibit chemical and structural variability that is unique among biopolymers. The functional versatility of polysaccharides in pharmaceutical practice is mostly associated with the modification of viscosity due to swelling. Theoretically, this property is related to the transition of glucose units of polymeric chains through a vast range of different energy states or conformations [6]. Because polysaccharides have numerous hydroxyl, acidic, and charged groups, they have a tendency to form regular or ordered structures such as single or multiple helices that are stabilized by hydrogen bonds, ionic bridges, and van der Waals interactions [7]. Conformational data on the Xan molecule are still questionable despite the fact that the numerous experimental methods have

Abbreviations: CRT, controlled-release technology; Xan, xanthan; AFM, atomic force microscopy.

* Corresponding author. Faculty of Pharmacy, University of Ljubljana, Aškerčeva 7, 1000 Ljubljana, Slovenia. Tel.: +386 1 476 9617; fax: +386 1 425 8031.
E-mail address: biljana.govedarica@ffa.uni-lj.si (B. Govedarica).

0939-6411/$ - see front matter © 2011 Elsevier B.V. All rights reserved.
doi:10.1016/j.ejpb.2011.09.008

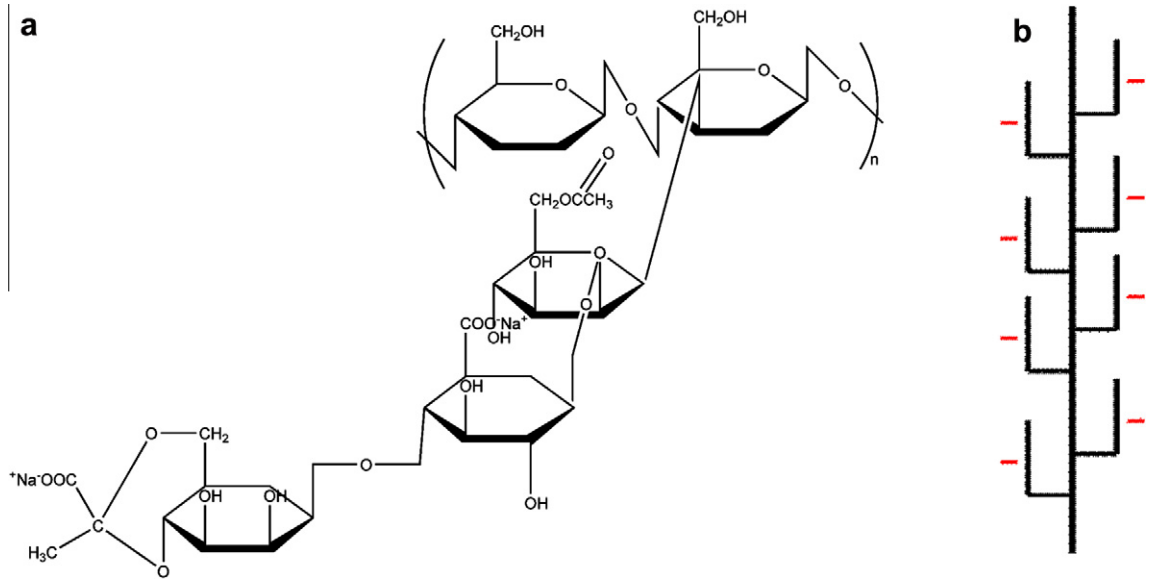

Fig. 1. (a) Structural formula of Xan; (b) schematic representation of Xan molecule. (For interpretation of the references to color in this figure legend, the reader is referred to the web version of this article.)

been used in the past 50 years. Some studies suggest a single helix (i.e., a disordered structure) [8–10] whereas others propose a double-stranded structure (i.e., an ordered conformation) [10–14]. However, still others claim that both conformations coexist, which contributes to difficulty in generalizing the secondary structure of Xan [15]. The most accepted evidence regarding its conformational transition from a double helix to a single one is the factor of two difference in the mass per length [11,13]. According to the literature data, the double-stranded structure exists in solution as a semi-rigid or rigid helix in which hydrogen bonding is the main type of interaction between the side chain and the main one. This structure can undergo a conformational change and become a single-helical structure if the ionic strength is reduced or the temperature is increased above the characteristic melting point [8].

A vast number of solution techniques have been performed in order to study the conformational structures of Xan, such as optical rotation, circular dichroism, light scattering, calorimetry, viscosity measurements, NMR, and size-exclusion chromatography [11,13, 16,17]. Due to the specific ability of polysaccharides to form aggregates in solutions, these techniques have mostly produced conflicting results regarding Xan's secondary structure. Moreover, due to the fact that the properties are measured at the bulk level, these techniques are likely to miss the characteristics of smaller subpopulations that deviate from the average [14]. In contrast, novel techniques can be used to investigate polymer structure in dilute solutions as well as the shape of the molecular chain. Theoretically speaking, polymer chains usually twist and create random, loose, three-dimensional coils that are a result of the chain's flexibility. Conformational analysis is required in order to elaborate polymer flexibility. This includes calculation of the following parameters: end-to-end distance, contour length, Kuhn segment, radius of gyration, and persistence length. Calculation of these parameters is well described in the literature [18–21].

For instance, changes in contour length due to the presence of ions or the influence of pH can induce helical transformation as noted by Camesano et al. [22]. Furthermore, polymer chain flexibility can be interpreted using the persistence length and the Kuhn segment. These two parameters provide a measure of the distance along which the polymer's direction persists before it changes course.

At the macroscale, the influence of helix–coil transition is evident from changes in the physical properties (e.g., viscosity, optical properties, etc.) of Xan solutions. It is known that the viscosity of a Xan solution does not change in the range of pH 3–10, but it dramatically decreases at pH values less than 3. Such a phenomenon is generally caused by a change in the molecular conformation [23].

Scanning probe microscopies, and especially atomic force microscopy (AFM), have been extensively used to study the molecular and supramolecular structures of biopolymers [24]. It is often preferable to perform very subtle AFM measurements in liquid even if measuring in air is feasible and acceptable. Imaging in organic solvents such as alcohols (e.g., 1-butanol, isopropanol, etc.) provides certain benefits in visualization of the polymers, such as minimizing the adhesion forces between the AFM tip and the molecule that can damage fragile biopolymers and inhibiting the polymer desorption from the surface, due to their precipitating effect [25].

The use of AFM to measure the length, thickness, and other physical properties of polymers is well established in the study of DNA [26]. Single molecular studies provide new insights into the microscopic basis of macroscopic polymer properties such as elasticity and degree of swelling. This study also presents AFM as an active micro-rheology technique for probing the mechanical properties of Xan films. Our intention was to evaluate the physical properties of crude (raw) Xan powder. Numerous studies have been carried out on thermally treated or purified Xan. It is well known from the literature that such treatment can induce conformational changes in biopolymers, which is unacceptable from the pharmaceutical point of view.

The results presented in this paper support our recently published work, in which we established that the medium's pH and ionic strength affect the swelling dynamics and gel formation of Xan matrix tablets and consequently influence the drug-release kinetics [27].

Therefore, the ultimate goal was to understand and be able to predict the swelling behavior of Xan tablets under various media conditions (different pH levels and ionic strengths) using data obtained from single molecules and films by AFM and other complementary techniques.

2. Materials and methods

2.1. AFM analysis of single Xan polymer chains

The commercial Xan sample (G1253) was supplied by Sigma–Aldrich of St. Louis, MO, USA, as a yellow-to-tan powder with the provided specifications (Mw = 4×10^6 g/mol and $[\eta]$ = 800–1200 mPa s for 1% solution). The powder was dispersed in media with various pH and ionic strengths as follows: distilled water (pH 7; μ = 0 M), HCl solution (pH 1.2; μ = 0.08 M), HCl solution (pH 3.0; μ = 0.001 M), and CH_3COONH_4 solution (pH 3.0; μ = 0.2 M). All Xan solutions were prepared in the concentrations of 1 g/L, gently stirred overnight and diluted with the media mentioned above in order to yield a final concentration of 0.2 mg/L (dilute Xan solution).

To freshly cleaved mica, 10 μl of dilute Xan solution was applied and left for 1–2 min in open air at room temperature. The liquid cell was positioned on the sample plate, and AFM imaging in 1-butanol was performed using a liquid imaging cell sealed with an O-ring. All measurements were performed using a Nanoscope III multimode scanning probe microscope equipped with an E-type scanner (Veeco, Santa Barbara, CA, USA). Silicon nitride cantilevers (MSCT, Veeco, Santa Barbara, CA, USA) with a spring constant of 0.1 N/m were used for imaging. Data were recorded at a scan rate of 3 Hz and stored in 512 × 512 pixel format. Images were processed using the Nanoscope software. For optimal image quality of structural details, second-order flattening was applied. For each condition, at least 30 individual polymer chains were analyzed.

Using 2D Single Molecule Software (Clarkson University, Potsdam, NY) contour lines of polymer chains were digitized into the pixels yielding the spatial coordinates of each position along the polymer. Only those chains meeting the following criteria were included in the calculation of the chain's dimensions: (a) both ends of the chain were visible; (b) the chain was not in contact with or crossed by any other chain.

From the image data, the parameters that describe the polymers in solutions, such as the root-mean-square radius of gyration, contour length, and end-to-end distance, were calculated. The persistence length was computed assuming the validity of worm-like-chain (WMC) model [28]. According to this model, the probability density function of the angle between consecutive links of the chain is Gaussian and can be interpreted using Eq. (1) [19]:

$$P(\theta(l)) = \left(\frac{L_p}{2\pi l}\right)^{\frac{1}{2}} \exp\left(\frac{L_p\theta^2}{2l}\right) \quad (1)$$

where θ is the bend angle, l is the distance between segments, and L_p is the persistence length of the polymer.

The persistence length is than calculated according to the following relationship (Eq. (2)):

$$\langle\theta^2(l)\rangle = \left(\frac{l}{L_p}\right) \quad (2)$$

To obtained θ as a function of l from the images, a series of equal length vectors (equals to about the pixel size in units of the image scale in nm) was projected into the digitized trace of the polymer contours. The angle θ between consecutive vectors was calculated over the length of the molecule. Since AFM is a surface technique, the fashion in which Xan molecules adhere to the surface must be addressed.

Kinetically trapped molecules reflect information contained in the 3D conformation of the polymer chains (opposite to equilibrium trapping in which the molecules are rearranged in the 2D manner). In this case, 3D angle θ between two segments during kinetic trapping will be preserved. Moreover, the Eq. (2) has already been applied in 3D manner by Bednar et al. [29] and Abels et al. [30].

Eventually, for the interpretation of the results and for the predictions of Xan behavior in the bulk (films), only 3D trapped polymer chains were considered.

2.2. Nanoindentation measurements

Xan was dissolved in the following media: distilled water (μ = 0 M), HCl solution (pH 1.2; μ = 0.08 M), HCl solution (pH 3.0; μ = 0.001 M), and NaCl solution (pH 7.0; μ = 0.2 M) in concentrations of 20 g/l and stirred overnight using a magnetic stirrer. The each solution (m = 5 g) was cast in matrices (equal size) on Teflon plates and dried under ambient conditions for 24 h. After drying, the transparent film was carefully peeled off the surface. The thickness of the film samples was measured using a micrometer (Mitutoyo, Kawasaki, Japan) and the mean thickness was calculated.

In order to evaluate the elastic properties of Xan films, nanoindentation measurements were performed by collecting the force curves on the investigated samples and cleaved mica as a non-deformable reference. AFM force spectroscopy was carried out on a NanoScope IIIa (Veeco, Santa Barbara, CA, USA) using silicon nitride cantilevers with pyramidal tips (PPP-FM, nominal spring constant 2.8 N/m, resonance frequency 75 kHz; Nanosensors, Wetzler, Germany). The spring constants (k) of the cantilevers were determined using the thermal noise method.

The indentation experiments on Xan films involved collecting the individual force curves from various locations on the scanned surface. Smaller areas (~500 nm) were focused before performing the nanoindentation experiments. These measurements provide the change in cantilever deflection as a function of probe displacement. The deflection vs. probe displacement curve was converted into force–deformation curves using the cantilever spring constant. The deformation can also be easily calculated by subtracting the deflection from the probe displacement. The error due to uncertainty in the contact point can be avoided if the force–deformation dependence is accounted for by taking the power of 2/3 of both sides of Eq. (3). The linear region was used to calculate the Young's modulus using the Hertz equation (Eq. (3)) [31]:

$$F = \frac{4\sqrt{R_c}}{3}\frac{E}{1-\nu^2}\delta^{3/2} \quad (3)$$

where F is the compressing force, δ is the deformation, R_c is the probe's radius of the curvature, E is the elastic modulus, and ν is the Poisson ratio of the elastic solid. A Poisson ratio of 0.5 was used for the calculation. During data processing, the appropriateness of the linear fit was estimated by calculating the coefficient of determination (r^2). The mean r^2 value of linear regression analysis was estimated separately for each sample. All force–distance curve experiments were performed at the same loading rate. At least 50 force curves were collected on each investigated sample.

2.3. Mechanical property measurements

The mechanical properties of Xan films were evaluated using a custom-made mechanical hardness meter. The strength tester and software were developed at the Department of Pharmaceutical Technology, University of Szeged. The device contains a special specimen holder (20 mm in diameter) and a hemisphere stamp with a surface of 201 mm^2. The instrument is connected to a computer via an interface, and the breaking force is measured. The round specimen is positioned horizontally, and the stamp moves vertically. The films were prepared in the same manner as for the nanoindentation measurements. A 50-mm film strip, free from air bubbles or physical imperfections, was held in a specially

designed ring sample holder. The breaking force was determined from the curves. Measurements were performed at least five times for each film.

2.4. Dissolution study

Xan and the drug (pentoxifylline, Krka, Novo Mesto, Slovenia) were mixed homogeneously using a laboratory model drum blender; 100 mg of pentoxifylline was directly compressed (SP 300, Kilian, Cologne, Germany) to form circular flat-faced tablets with a mass of 0.50 g ± 0.01 g, a diameter of 12 mm, and a crushing strength of 100 ± 10 N. Dissolution tests were performed on a fully calibrated dissolution apparatus using the redesigned paddle method (VanKel Dissolution Apparatus, VK 7000, Cary, NC, USA). The measurement settings were the following: 50 rpm (paddle speed), temperature 37 °C ± 0.5 °C, and 900 ml medium volume. At predetermined time intervals, 10 ml samples were withdrawn without being replaced. The collected samples were filtered through 10 μm filters, suitably diluted with the release medium, and the absorbance was measured spectrophotometrically at 274 nm (HP Agilent 8453 Diode Array UV–VIS Spectrophotometer, Waldbronn, Germany). Experiments were performed in six media: water (μ = 0 M), water + NaCl (μ = 0.2 M), HCl (pH 1.2; μ = 0.08 M), HCl (pH 1.2) + NaCl (μ = 0.28 M), HCl (pH 3.0; μ = 0.001 M), and HCl (pH 3.0) + NaCl (μ = 0.201 M). Finally, analysis of the influence of medium replacement simulating physiological conditions on the release of pentoxifylline from Xan tablets was performed.

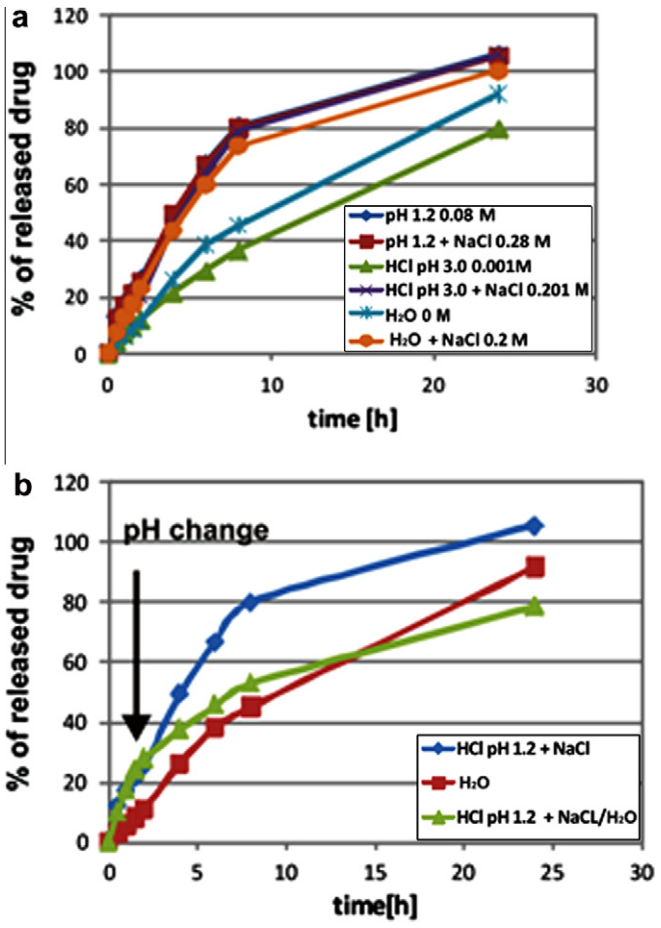

Fig. 2. (a) Release profiles of pentoxifylline from Xan tablets in various media; (b) the influence of medium replacement (denoted by arrow) simulating physiological conditions on the release of pentoxifylline from Xan tablets: HCl (pH 1.2) + NaCl medium was replaced after 2 h by water. For comparison, release of pentoxifylline from Xan in water and in HCl (pH 1.2) + NaCl is presented.

3. Results

3.1. Dissolution study

A dissolution test was conducted as a standard method for determining the drug release rate from Xan matrix tablets. The release rate differences observed were the main reason for carrying out AFM, as well as other complementary techniques, in order to discover the basic reason for such behavior.

Before pentoxifylline diffuses out of the matrix, water has to penetrate the polymer matrix, leading to polymer swelling and drug dissolution. The enhanced mobility of the polymeric chains favors the transport of water, drug dissolution, and the drug's diffusion out of the tablets. However, the arrangement of water molecules within hydrophilic polymers is very important because it influences the formation of the polymeric gel network and therefore also drug diffusion.

Our results demonstrate a slow dissolution rate of pentoxifylline from Xan matrix tablets in media such as water and HCl (pH 3.0). Increasing the ionic strength significantly accelerated the dissolution rate of the model drug (Fig. 2a).

The results of drug release performed under simulated physiological conditions, in which the HCl (pH 1.2) medium was replaced with water, proved that not only the gel layer thickness, but also the drug release rate from Xan tablets responds quickly to altered environmental conditions (Fig. 2b). The release is much faster during the first 2 h than after the replacement of the medium, when a gradually decreasing dissolution rate was observed. From this result, it can be concluded that swelling and consequently drug release from Xan tablets will be distinct in the stomach and intestinal environments.

3.2. AFM single molecule study

The appearance of Xan chains adsorbed on the surface of mica depends on the solvent medium used to prepare the sample. Sample preparation is the crucial issue for this microscopy technique when the aim is to visualize the individual molecules. In order to avoid aggregation artifacts in Xan samples for AFM imaging, very low concentrations of polymer (0.2 mg/l) in media of different ionic strengths and pH were used. Because the range of ionic strengths in gastrointestinal fluid is from 0.01 to 0.166 M [32], the ionic strengths of solutions were adjusted from 0 to 0.20 M using HCl or CH_3COONH_4. The characteristic appearances of single polymer chains surface-adsorbed from different solutions are presented in Fig. 3.

The images of samples prepared in these media reveal elongated polymer chains with occasional loops (Fig. 3d) and bifurcations (Fig. 3c and e). According to the literature, these loops are attributed to the existence of a single-helical structure or unraveling of a double or triple helix into a single one [20].

Furthermore, some knots (Fig. 3b) can also be observed. Knots are present at specific sites where intermolecular associations can occur and they are usually attributed to apolar contaminants such as the acetate groups.

The measured heights of the Xan's chains in media with low (H_2O and HCl pH 3.0) and high ionic strengths (HCl pH 1.2 and CH_3COONH_4 pH 3.0) are 0.6 ± 0.1 nm and 1.3 ± 0.2 nm, respectively (Fig. 3g and e). Due to the insufficient resolution of AFM images and small helical pitch [33] of the Xan's molecule (4.9 nm), the helical structure was not visualized. However, the conformational transition is supported by the chain's height being two times

greater in media with higher ionic strength compared to water and HCl (pH 3.0).

3.3. Chain statistics

Reconstruction of the Xan conformation was performed using a 2-D image analysis based on the work of Frontali et al. [19]. The heterogeneity of the sample can be assessed using the AFM images and can be quantitatively confirmed by the large standard deviations of our results. The contour lengths of the Xan molecules decreased in the progression from water to solutions with higher ionic strengths or low pH (HCl 1.2) (see Fig. 4).

Persistence length is a basic mechanical property quantifying the stiffness of a long polymer. It is sometimes defined as the polymer's resistance to bending. Our results, presented in Fig. 5, demonstrate the decreasing persistence length with increasing ionic strength. Longer chains of Xan as observed in water and HCl (pH 3.0) behave more like wormlike coils in contrast to shorter chains, in which the contour length is almost comparable with the persistence length and the structure is rigid and rod-like. Our experimental results are in agreement with the other literature data

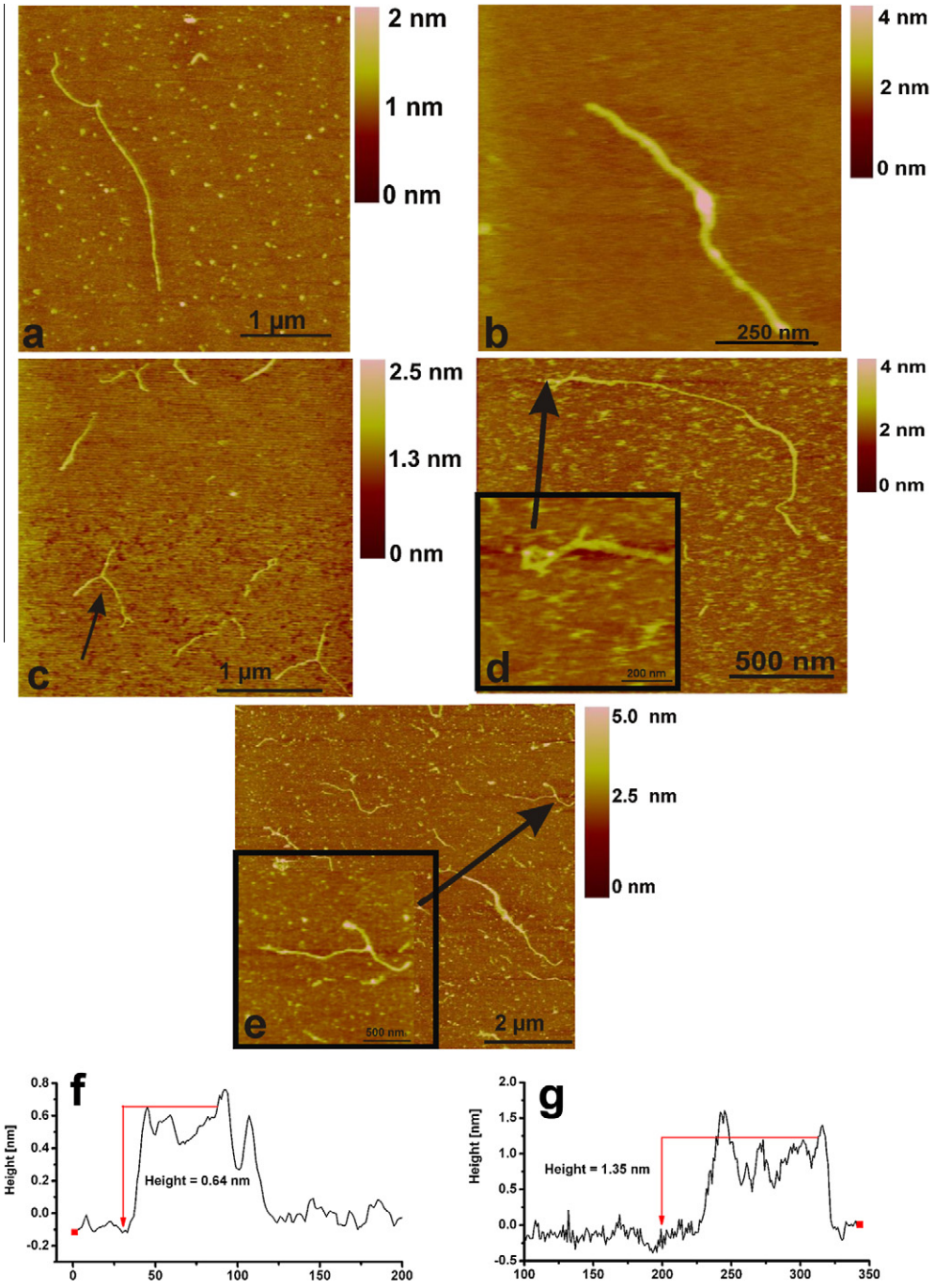

Fig. 3. Xan's polymer chains in water (μ = 0 M) (a); HCl pH 1.2 (μ = 0.08 M) solution (b); HCl pH 3.0 (μ = 0.001 M) solution (c) bifurcation can be visualized; HCl pH 3.0 (μ = 0.001 M) solution (d) loops can be observed (magnification); CH_3COONH_4 pH 3.0 (μ = 0.2 M) solution – bifurcation can be observed (magnification) (e); cross-section of Xan's chain in water (height 0.6 ± 0.1 nm) (f); cross-section of Xan's chain in HCl pH 1.2 (height 1.3 ± 0.2 nm) (g). (For interpretation of the references to color in this figure legend, the reader is referred to the web version of this article.)

regarding Xan contour and persistence lengths as obtained by AFM image analysis [21,22,24,34].

The presence of ions reduces the strong intermolecular electrostatic repulsion due to the presence of a negative charge in the Xan side chain. This can allow intensive bending of the polymer chain and consequently a decrease in the persistence length. Larger values for the persistence lengths in media with lower ionic strength (H_2O and HCl pH 3.0) explain the high viscosity of gels in swollen Xan matrix tablets [27] and consequently slower dissolution rates of the incorporated drug.

According to our results, the conformational transition from a single helix to double one is additionally supported by decreasing the contour and persistent length by adding salt or ions.

Because the end-to-end distance is difficult to measure, the radius of gyration is commonly utilized to define the average distance from the center of gravity to the chain segment (Fig. 6).

The measured radius of gyration (Fig. 7) clearly demonstrates that this parameter decreases with increasing ionic strength of the solution.

The increased gyration radii in media with low ionic strengths denote hydration of the polymer chains that is macroscopically observed as an abundant swelling of the matrix. In contrast, in the presence of ions, polymers do not swell to a great extent, and there are larger regions of low microviscosity, which results in an increase in the free volume due to the presence of micropores (smaller gyration radii). In this sense, a shift in the dissolution rate can be observed. Furthermore, the increase in the gyration radii in H_2O and HCl (pH 3.0) indicates more entangling of Xan chains and consequently a reduction in the pore size in the gel. This reduction in pore size results in a slower dissolution rate from Xan matrix tablets in media with low ionic strengths, which is evident from the dissolution test (Fig. 2).

Polymer entanglement seems to be the preferred mode of molecular association, even in dilute solutions. For example, this phenomenon has been utilized to explain the shear dependence of tear viscosity [35]. The differences in the dissolution rates in various media may be therefore a consequence of the ability of the polymer to entangle and create pores in the structure of a gel.

3.4. Nanoindentation measurements

Nanoindentation measurements were performed in order to determine the stiffness of the overall composite structure of a polymeric film that contains contribution from the individual polymer chains.

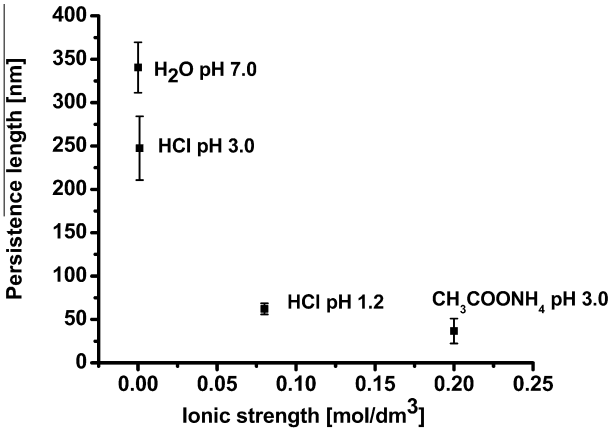

Fig. 5. Persistence length of Xan as a function of the ionic strength of the medium. Persistence length was calculated from the bend angle and the distance between segments using single molecular image analysis. At least 30 individual molecules in 3D equilibrium were used to obtain a mean value for the persistence length.

In addition to obtaining high-resolution images of molecules adsorbed to the surface, the utilized cantilevers can serve as soft indenters permitting the local mapping of the elasticity of the sample surface. Generally, polymers are evaluated by their degree of swelling after absorbing a defined amount of water. In such a case, the main measure of the stiffness of an isotropic elastic material, or Young's modulus, is dependent on the degree of swelling in a given medium. This correlation can be mathematically interpreted under defined conditions (e.g., constant temperature and degree of cross-linking) using Eq. (4) [36]:

$$E \approx A\left(\frac{V}{V_0}\right)^{-\frac{5}{3}} \tag{4}$$

where E is the Young's modulus, V/V_0 is the degree of swelling relative to the initial volume of the polymer (V_0), and A is a constant. Eq. (4) expresses a reciprocal relationship between the Young's modulus and the degree of swelling. Differences in the dissolution rates of the drug ingredient (from the tablets) were clarified using this equation.

The force–deformation relationship can be represented by the Hertz model. In spite of some limitations of this model [37], it is still useful for evaluating the mechanical properties of various samples.

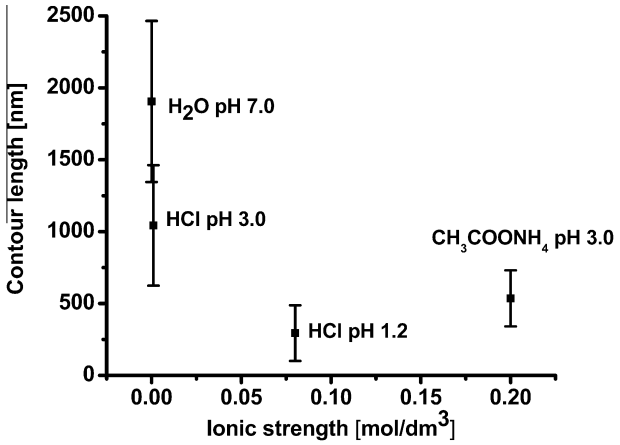

Fig. 4. Contour length dependence of Xan polymer chains as a function of ionic strength. The contour lengths were determined using a single molecular imaging method and average values of at least 30 molecules were taken into account.

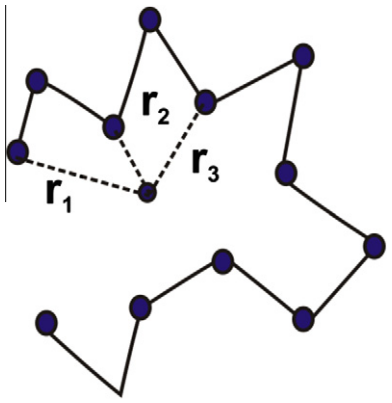

Fig. 6. Radius of gyration: r_1, r_2, and r_3 are the average distance of a monomer from the polymer's center of mass. (For interpretation of the references to color in this figure legend, the reader is referred to the web version of this article.)

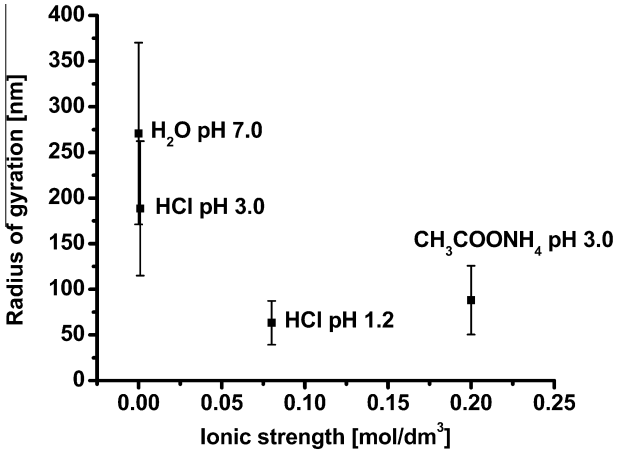

Fig. 7. Radius of gyration of Xan as a function of the ionic strength. The radius of gyration is a geometrical calculation and for polymers coils can be computed according to the mean-square value of the end-to-end distance.

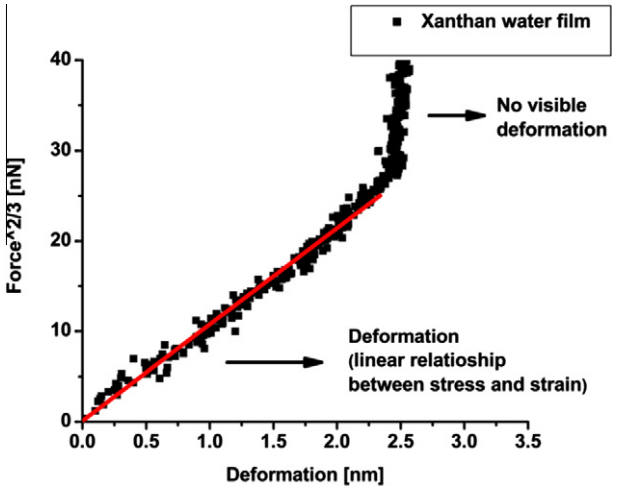

Fig. 8. The force–deformation curve obtained using AFM force spectroscopy on Xan film prepared from a water solution. (For interpretation of the references to color in this figure legend, the reader is referred to the web version of this article.)

There are some issues that should be kept in mind, such as the fit range and composition of the sample in order to yield reasonable and reproducible results. It is worth noting that the Hertz model is valid only for small indentation depths in which the substrate cannot affect the calculations [28]. The elasticity of the sample is determined from the first part of the curve, which represents a linear relationship between the force to the power of 2/3 and the deformation, compared to the part of the curve where no deformation is visible, representing the stiffness of the substrate surface (Fig. 8).

As a rule of thumb, it should be kept in mind that the stiffness of the cantilever should be close to the stiffness of the sample. Accordingly, we utilized soft cantilevers to determine the Young's modulus of the polymeric films. In order to account for the Hertz model limitations regarding substrate influence, we prepared films more than 90-μm thick, which exceeds the maximum indentation.

Fig. 9 shows the histograms of the Young's moduli for various Xan films. Films made from solutions with lower ionic strength show greater elasticity than films prepared in HCl (pH 1.2) and NaCl solution.

The neutralization of COO^- groups in pH 1.2 or electrophilic shielding by NaCl is probable reasons for the re-association of the hydrogen bonds that contributes to the enhanced rigidity of

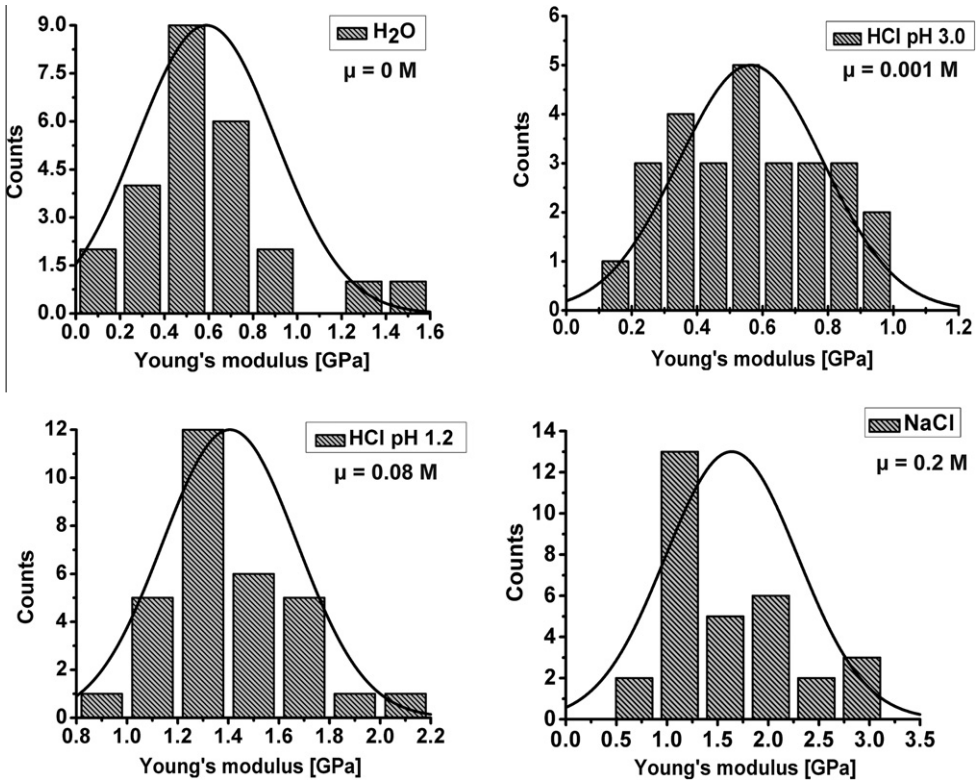

Fig. 9. Histograms of Young's modulus for various Xan films from water, HCl (pH 3.0), HCl (pH 1.2), and NaCl ($\overline{E}(H_2O) = 0.6 \pm 0.3$ GPa; $\overline{E}$(HCl pH3.0) $= 0.69 \pm 0.2$ GPa; $\overline{E}$(HCl pH1.2) $= 1.4 \pm 0.3$ GPa; $\overline{E}$(NaCl) $= 1.6 \pm 0.7$ GPa).

these films (a larger Young's modulus) and lower swelling capacity (Eq. (4)). Subsequently, this lower swelling capacity restricted the formation of abundant gel layer on tablet surface, thus increased dissolution rate of the model drug from Xan matrix tablets is observed and confirmed by the dissolution test (Fig. 2).

On the other hand, in solutions with lower ionic strengths as well as neutral media such as water, these COO^- groups are deionized and cause breakage of the hydrogen bonds. Faster water ingress allows hydration of polymer chains and swelling of the matrix. According to Eq. (4), a larger degree of swelling is accompanied by a lower Young's modulus of such films (Fig. 9) and is related to slower release rate of the incorporated drug (Fig. 2).

The AFM nanoindentation data were also compared with the measurements of the breaking forces of Xan polymer films determined with a mechanical hardness meter. Xan films prepared in water, HCl (pH 1.2), and NaCl solution were chosen for the mechanical property evaluation. Table 1 shows the collected results of these measurements. It can be clearly observed that the Xan films prepared from solutions with higher ionic strength exhibit significantly higher breaking forces compared with the film prepared in water. These data correspond very well to the Young's moduli obtained for the same films using AFM.

3.5. Single vs. bulk correlations

Fig. 10a represents the correlation between microscopic polymer property such as radius of gyration and macroscopic characteristic such as the film thickness. According to our results, polymer's radius of gyration is controlling factor of the film thickness, which is verified from the strong linear correlation between these two parameters (Fig. 10a). This is explained by the radius of gyration effect on polymer packing in the structure of the film. Radius of gyration gives a sense of the size of the polymer chains. Therefore, in media with higher ionic strength, reduced radius of gyration is related to smaller polymer size. Consequently, this contributes to closer packing of the polymer chains and reduced film thickness. Moreover, minimized electrostatic repulsion between the individual polymers chains in such media provides also closer organization of the polymer chains in the final structure of the film. On the other hand, loose and more prominent Xan's films are observed in media such as H_2O and HCl pH 3.0 due to increased steric exclusion (more extended Xan chains – larger radius of gyration) and increased electrostatic repulsion between individual polymer molecules.

Decreasing of the film thickness with the increasing of the solution ionic strength has already been observed in the literature [38]. Nevertheless, our study provide experimental data (radius of gyration) in order to elucidate ionic strength effect on polymer film thickness.

Even more, observed correlation excellently corresponds to another bulk property such as increased gel layer thickness in swelled Xan's matrix tablets, according to our recently published results in which magnet resonance imaging was performed for dynamic observation of Xan's tablets swelling behavior [27].

Table 1
Breaking forces for Xan films.

Xanthan films (20 g/L)	Ionic strength (M)	Breaking force (N)	Film thickness (mm)
Water	0	3.2 ± 1.5	0.18 ± 0.05
HCl (pH 3.0)	0.001	3.3 ± 1.4	0.15 ± 0.08
HCl (pH 1.2)	0.08	10.4 ± 3.4	0.05 ± 0.008
NaCl	0.2	12.7 ± 3.0	0.09 ± 0.02

The relationship between another micro- (persistence length) and macroscopic parameter (Young's modulus of Xan's film) is demonstrated in Fig. 10b.

Variations in the Young's modulus of the Xan's films prepared from the solutions with different ionic strength can be predicted by calculating the molecular persistence length (Fig. 10b). For instance, smaller persistence length of individual polymer chains is ascribed to more compact and stiffer structure of Xan's films (larger Young's modulus) in media with higher ionic strengths. The obtained correlation is in agreement with the inversely interpreted relationship between these intrinsic properties, according to the literature data [39].

4. Conclusion

Here, we introduced sample preparation, single molecular imaging, and data analysis technique in conjunction with nanomechanical testing to gain insights into the importance of single polymer properties for the prediction of the bulk attributes such as swelling and dissolution rate from Xan's matrix tablets. We successfully come to the conclusion that microscopic polymer properties such as radius of gyration and persistence length are responsible for the macroscopic polymer behavior.

For example, longer persistence lengths and radius of gyration of Xan's chains result in a higher degree of swelling, corresponding

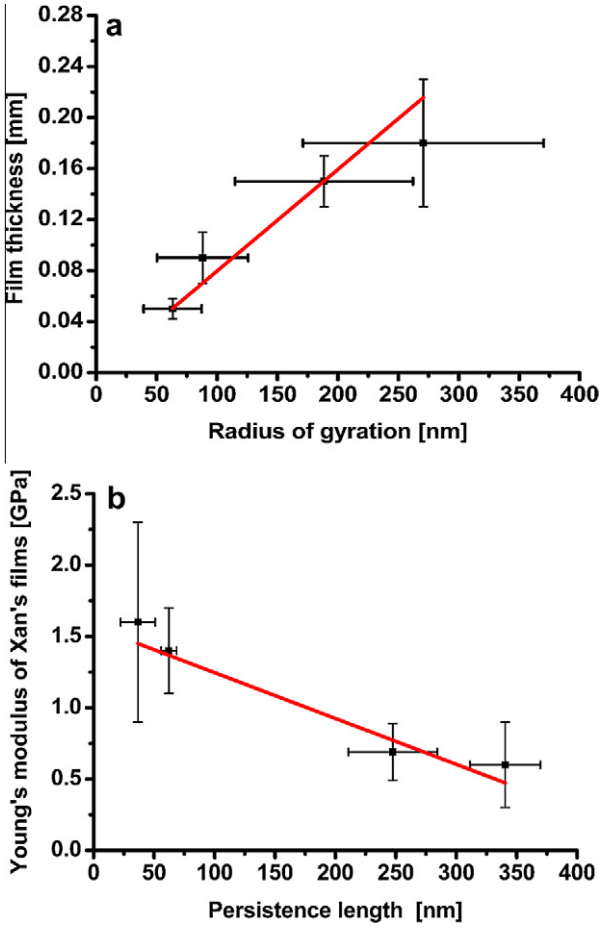

Fig. 10. (a) Film thickness vs. radius of gyration of Xan molecules in media with different ionic strength; (b) relationship between Young's modulus of Xan's films and molecular persistence length in media with different ionic strengths. (For interpretation of the references to color in this figure legend, the reader is referred to the web version of this article.)

to softer polymer films, increased gel layers in matrix and a slower release rate of the incorporated drug from the tablets.

We expect that quantification of the intrinsic properties of polymers on a single and bulk scale is important in pre-formulation study of polymer matrix systems for several reasons. First of all, it gives data of physical and mechanical properties of polymers used for the preparation of matrix tablets. Furthermore, it provides a possibility to relatively predict dissolution rates without involving the time and material-consuming dissolution test in pre-formulation phase of product design. Moreover, it offers the basis for understanding of the dissolution rates of final tablet products.

Acknowledgment

The authors express special thanks to research assistant professor Yuri Roiter from the Clarkson University, Department of Chemistry and Biomolecular Science, New York, for providing the Single Molecule Software.

References

[1] R. Langer, N. Peppas, Present and future applications of biomaterials in controlled drug delivery system, Biomaterials 2 (1981) 201–214.
[2] B. Katzbauer, Properties and applications of xanthan gum, Polym. Degrad. Stab. 59 (1998) 81–84.
[3] P.E. Jansson, L. Kenne, B. Lindberg, Structure of extracellular polysaccharide from *Xanthomonas campestris*, Carbohydr. Res. 45 (1975) 275–282.
[4] L.D. Melton, L. Mindt, D.A. Rees, G.R. Sanderson, Covalent structure of the extracellular polysaccharide from *Xanthomonas campestris*: evidence from partial hydrolysis studies, Carbohydr. Res. 46 (1976) 245–257.
[5] H. Yanai, T. Sato, Local conformation of the cellulosic chain in solution, Polym. J. 38 (2006) 226–233.
[6] D. Brant, Versatile Polysaccharides: Ropes, Rings and Rods, 2005. <http://www.bbcm.univ.trieste.it/~cesaro/brant/lectio.pdf> (25.06.2011).
[7] Q. Zhang, P.E. Marszalek, Solvent effects on the elasticity of polysaccharide molecules in disordered and ordered states by single-molecule force spectroscopy, Polymer 47 (2006) 2526–2532.
[8] I. Capron, G. Brigand, G. Muller, About the native and renatured conformation of xanthan exopolysaccharide, Polymer 38 (1997) 5289–5295.
[9] I.T. Norton, D.M. Goodall, S.A. Frangou, E.R. Morris, D.A. Rees, Mechanism and dynamics of conformational ordering in xanthan polysaccharide, J. Mol. Biol. 175 (1984) 371–394.
[10] G. Holzwarth, E. Prestridge, Multistranded helix in xanthan polysaccharide, Science 197 (1977) 757–759.
[11] G. Paradossi, D.A. Brant, Light scattering study of a series of xanthan fractions in aqueous solution, Macromolecules 15 (1982) 874–879.
[12] T. Sato, T. Kakihara, A. Teramoto, Isotropic-liquid crystal phase equilibrium in semiflexible polymer solutions: xanthan, a rigid polyelectrolyte, Polymer 5 (1990) 824–828.
[13] A. Gamini, M. Mandel, Physicochemical properties of aqueous xanthan solutions: static light scattering, Biopolymers 34 (1994) 783–797.
[14] I. Capron, S. Alexandre, G. Muller, An atomic force microscopy study of the molecular organisation of xanthan, Polymer 39 (1998) 5725–5730.
[15] B.T. Stokke, A. Elgsaeter, O. Smidsrod, Electron microscopic study of single-and double-stranded xanthan, Int. J. Biol. Macromol. 8 (1986) 217–225.
[16] V.J. Morris, D. Franklin, K. I'Anson, Rheology and microstructure of dispersions and solutions of the microbial polysaccharide from *Xanthomonas campestris* (xanthan gum), Carbohydr. Res. 121 (1983) 13–30.
[17] M . Milas, M. Rinaudo, R. Duplessix, R. Borsali, P. Lindner, Small angle neutron scattering from polyelectrolyte solutions: from disordered to ordered xanthan chain conformation, Macromolecules 28 (1995) 3119–3124.
[18] H. Li, T.A. Witten, Fluctuations and persistence length of charged flexible polymers, Macromolecules 28 (1995) 5921–5927.
[19] C. Frontali, E. Dore, A. Ferrauto, E. Gratton, A. Bettini, M.R. Pozzan, et al., An absolute method for the determination of the persistence length of native DNA from electron micrographs, Biopolymers 18 (1979) 1353–1373.
[20] A.R. Kirby, P. Gunning, V.J. Morris, Imaging xanthan gum by atomic force microscopy, Carbohydr. Res. 267 (1995) 161–166.
[21] M. Rinaudo, Relation between the molecular structure of some polysaccharides and original properties in sol and gel states, Food Hydrocolloids 15 (2001) 433–440.
[22] T.A. Camesano, K.J. Wilkinson, Single molecule study of xanthan conformation using atomic force microscopy, Biomacromolecules 2 (2001) 1184–1191.
[23] M.M. Talukdar, R. Kinget, Swelling and drug release behaviour of xanthan gum matrix tablets, Int. J. Pharm. 120 (1995) 63–72.
[24] T.M. McIntire, D.A. Brant, Imaging of individual biopolymers and supramolecular assemblies using noncontact atomic force microscopy, Biopolymers 8 (1997) 133–146.
[25] A. Alessandrini, P. Facci, AFM: a versatile tool in biophysics, Meas. Sci. Technol. 16 (2005) R65–R92.
[26] D.I. Cherny, A. Fourcade, F. Svinarchuk, P.E. Nielsen, C. Malvy, E. Delain, Analysis of various sequence-specific triplexes by electron and atomic force microscopies, Biophys. J. 74 (1998) 1015–1023.
[27] U. Mikac, A. Sepe, J. Kristl, S. Baumgartner, A new approach combining different MRI methods to provide detailed view on swelling dynamics of xanthan tablets influencing drug release at different pH and ionic strength, J. Control. Release 145 (2010) 247–256.
[28] O. Kratky, G. Porod, Rontgenuntersuchung gelosre faden-molekule, Recl. Trav. Chim. Pays-Bas. 68 (1949) 1106.
[29] J. Bednar, P. Furrer, V. Katritch, Z. Stasiak, J. Dubochet, A. Stasiak, Determination of DNA persistence length by cryo-electron microscopy. Separation of the static and dynamic contributions to the apparent persistence length of DNA, J. Mol. Biol. 254 (1995) 579–594.
[30] J. Abels, F. Moreno-Herrero, T. van der Heijden, G. Dekker, N. Dekker, Single-Molecule measurements of the persistence length of double-stranded RNA, Biophys. J. 88 (2005) 2737–2744.
[31] H. Hertz, Über die Berührung fester elastischer Körper, J. reine angew. Math. 92 (1826) 156–171.
[32] J. Johnson, J. Holinej, M. Williams, Influence of ionic strength on matrix integrity and drug release from hydroxypropyl cellulose compacts, Int. J. Pharm. 90 (1993) 151–159.
[33] T. Sho, T. Sato, T. Norisuye, Viscosity behaviour and persistence length of sodium xanthan in aqueous sodium chloride, Biophys. Chem. 25 (1986) 307–313.
[34] V. Parpura, J.M. Fernandez, Atomic force microscopy study of the secretory granule lumen, Biophys. J. 71 (1996) 2356–2366.
[35] M. Radmacher, M. Fritz, P. Hansma, Imaging soft samples with the atomic force microscope: gelatin in water and propanol, Biophys. J. 69 (1995) 264–270.
[36] W. Winter, Polysaccharide structure by X-ray fiber diffraction, Methods Enzymol. 83 (1982) 87–104.
[37] J.M. Tiffany, Viscoelastic properties of human tears and polymer solutions, Adv. Exp. Med. Biol. 350 (1994) 267–270.
[38] K.S. Sorbie, Y. Huang, The effect of pH on the flow behavior of xanthan solution through porous media, J. Colloid Interf. Sci. 149 (1991) 303–313.
[39] H. Morawetz, Macromolecules in Solution, Wiley, New York, 1975.